Biochemical Pharmacology 79 (2010) 587–595

Contents lists available at ScienceDirect

Biochemical Pharmacology

journal homepage: www.elsevier.com/locate/biochempharm

Predicting gemcitabine transport and toxicity in human pancreatic cancer cell lines with the positron emission tomography tracer 3′-deoxy-3′-fluorothymidine

Robert J. Paproski [a,b], James D. Young [b,c], Carol E. Cass [a,b,*]

[a] Department of Oncology, University of Alberta, Cross Cancer Institute, 11560 University Ave., Edmonton, Alberta, Canada T6G 1Z2
[b] Membrane Protein Research Group, University of Alberta, Edmonton, Alberta, Canada
[c] Department of Physiology, University of Alberta, 7-25A Medical Sciences Building, Edmonton, Canada T6G 2H7

ARTICLE INFO

Article history:
Received 5 August 2009
Accepted 23 September 2009

Keywords:
Gemcitabine
3′-Deoxy-3′-fluorothymidine
hENT1
Nucleoside transporters
Predicting toxicity

ABSTRACT

The abundance of human equilibrative nucleoside transporter 1 (hENT1) has recently been shown to be a predictive marker of benefit from gemcitabine therapy in patients with pancreatic cancer. Since hENT1 is also important for the uptake of positron emission tomography (PET) tracer 3′-deoxy-3′-fluorothymidine (FLT) in various cultured human cell lines, this study was undertaken to determine if FLT uptake predicts gemcitabine uptake and/or toxicity in a panel of human pancreatic cancer cell lines (Capan-2, AsPC-1, BxPC-3, PL45, MIA PaCa-2, and PANC-1). Capan-2 cells displayed the lowest levels of (1) extracellular nitrobenzylmercaptopurine ribonucleoside (NBMPR) binding, which represents cell-surface hENT1, (2) FLT and gemcitabine uptake during short (1–45 s) and prolonged (1 h) periods, and (3) gemcitabine sensitivity. Exposure to NBMPR (inhibits only hENT1) or dilazep (inhibits hENT1 and hENT2) reduced FLT and gemcitabine uptake and gemcitabine sensitivity, with dilazep having greater effects than NBMPR. Gemcitabine permeation was almost completely mediated, primarily by hENT1 and to a lesser extent by hENT2, whereas FLT permeation included a substantial component of passive diffusion. In five of six cell lines, correlations were observed between (1) FLT and gemcitabine initial rates of uptake, (2) gemcitabine uptake and gemcitabine toxicity, (3) FLT uptake and gemcitabine toxicity, and (4) ribonucleotide reductase subunit M1 expression and gemcitabine toxicity. FLT and gemcitabine uptake were comparable for predicting gemcitabine toxicity in the tested pancreatic cancer cell lines suggesting that FLT PET may provide clinically useful information about tumor gemcitabine transport capacity and sensitivity.

1. Introduction

Advanced pancreatic cancer is currently considered an incurable disease with median survival less than 1 year [1]. The standard treatment is single-agent gemcitabine, and, with the exception of erlotinib [2], other anticancer therapies have not shown any additional survival advantage when coupled with gemcitabine. As a cytidine nucleoside analog, gemcitabine requires human nucleoside transporters (hNTs) to cross plasma membranes of tumor cells before it is phosphorylated by deoxycytidine kinase (dCK) [3]. Recent studies suggest that pancreatic tumor levels of human equilibrative nucleoside transporter 1 (hENT1), as measured by immunohistochemistry, can be used to predict tumor response to gemcitabine. Patients with pancreatic tumors with abundant hENT1 display longer survival than those with tumors with undetectable or low levels of hENT1 [4,5].

hNTs are capable of transporting physiological nucleosides and many different therapeutic nucleoside analogs across cellular membranes (see Refs. [6–8] for hNT reviews). Gemcitabine can be transported by members of both hENTs (SLC29 family) and human concentrative nucleoside transporters (hCNTs, SLC28 family).

hENTs mediate bidirectional transport of nucleosides across biological membranes and are considered ubiquitous throughout the body. The four hENT family members include hENT1/2/3/4 and all hENTs, except hENT3, are considered plasma membrane transporters [9–12]. Both hENT1 and hENT2 have similar permeant selectivities, transporting purine and pyrimidine nucleosides as well as many synthetic nucleosides, although hENT2 (unlike hENT1) also transports some nucleobases. Among hNTs, hENT1 can be functionally identified by its sensitivity to inhibition by nitrobenzylmercaptopurine ribonucleoside (NBMPR) at nanomolar concentrations and hENT1/2 by their sensitivities to inhibition by dilazep at micromolar concentrations [11,12]. Both hENT1 and

* Corresponding author at: Department of Oncology, University of Alberta, Cross Cancer Institute, 11560 University Ave., Edmonton, Alberta, Canada T6G 1Z2.
Tel.: +1 780 432 8763; fax: +1 780 432 8886.
E-mail addresses: robertpa@cancerboard.ab.ca (R.J. Paproski), james.young@ualberta.ca (J.D. Young), carol.cass@cancerboard.ab.ca (C.E. Cass).

0006-2952/$ – see front matter © 2009 Elsevier Inc. All rights reserved.
doi:10.1016/j.bcp.2009.09.025

hENT2 transport gemcitabine although hENT1 displays a lower K_m value (i.e., higher affinity) for gemcitabine than hENT2 [13]. hENT3 is an intracellular pH-dependent, broadly nucleoside-selective transporter [9,14]. N-terminal deleted hENT3 produced in *Xenopus laevis* oocytes exhibits pH-dependent interaction with gemcitabine, suggesting that hENT3 may transport gemcitabine across intracellular membranes [14]. hENT4 displays pH-dependent adenosine-selective transport and is unlikely to be involved in gemcitabine transport [10].

hCNTs are nucleoside/cation symporters that concentrate nucleosides within cells by coupling the transport of nucleosides and cations down the cationic electrochemical gradient. The three hCNT family members (hCNT1/2/3) are all considered plasma membrane transporters [15–17]. hCNT1 is pyrimidine nucleoside-selective and hCNT2 is purine nucleoside-selective, although both transporters transport both adenosine and uridine [16,17]. hCNT3 has broad nucleoside selectivity, efficiently transporting both purine and pyrimidine nucleosides [15]. Gemcitabine, a pyrimidine nucleoside, is transported by hCNT1 and hCNT3 but not by hCNT2 [13,18].

Since hENT1 abundance has been shown by immunohistochemical staining of tumor samples to be a predictive marker for gemcitabine response in patients with pancreatic cancer, a non-invasive method for *in vivo* identification of pancreatic cancers with low gemcitabine transport capacity would be useful in predicting clinical resistance to gemcitabine. The positron emission tomography (PET) tracer 3′-deoxy-3′-fluorothymidine (FLT), a pyrimidine nucleoside analog, may be a probe for tumor gemcitabine transport capacity since FLT is transported by the same hNTs (hENT1, hENT2, hCNT1, and hCNT3) as gemcitabine [19].

Upon entering cells, FLT is phosphorylated by thymidine kinase 1 (TK1), a cell cycle specific kinase that has increased expression during S-phase [20]. Phosphorylated forms of FLT are not transported by hNTs and are therefore trapped within cells. FLT, which preferentially accumulates in proliferating cells with high TK1 activities, is used clinically as a PET proliferation tracer [21].

The present study was undertaken to determine if FLT transport and uptake could predict gemcitabine transport and toxicity in six human pancreatic cancer cell lines. The results demonstrated that hENT transport inhibitors significantly reduced (1) gemcitabine and FLT transport and uptake, and (2) gemcitabine toxicity in all six cell lines. In five cell lines, there were significant positive correlations between FLT and gemcitabine initial rates of uptake and between FLT uptake and gemcitabine toxicity. Measurements of FLT and gemcitabine uptake were comparable for predicting gemcitabine toxicity, suggesting that [^{18}F]FLT PET of pancreatic cancers may be useful clinically to predict gemcitabine sensitivity in patients.

2. Materials and methods

2.1. Cell culture

The pancreatic cell lines Capan-2, AsPC-1, BxPC-3, PL45, MIA PaCa-2, and PANC-1 used in this study were obtained from the American Type Culture Collection (Manassas, VA). Unless otherwise indicated, all cell culture reagents were obtained from Gibco (Carlsbad, CA).

AsPC-1, BxPC-3, and PL45 were maintained in RPMI 1640 medium containing 10% (v/v) fetal bovine serum (FBS). MIA PaCa-2 and PANC-1 cells were maintained in Dulbecco's modified Eagle's medium (DMEM) with 10% (v/v) FBS and Capan-2 cells were maintained in McCoy's 5A medium with 10% (v/v) FBS. For all binding and uptake experiments, cells were plated on 24-well plates (BD Falcon, Franklin Lakes, NJ) at 1×10^5 cells/well. For gemcitabine toxicity experiments, cells were plated on 96-well plates (Corning, Lowell, MA) at 5×10^3 cells/well. Plated cells were incubated at 37 °C with 5% CO_2 for 24 h at which point cells were used for equilibrium binding or uptake assays.

2.2. TaqMan real-time polymerase chain reaction (PCR)

Real-time PCR was performed as previously described [19] and all kits were used following manufacturers' instructions. Briefly, RNA from cell lines was isolated using the RNeasy kit (Qiagen, Hilden, Germany) and RNA was reverse transcribed into DNA using the TaqMan Gold RT-PCR kit (Applied Biosystems, Carlsbad, CA). For each real-time PCR reaction, cDNA was added to 2x TaqMan Universal PCR Master Mix (Applied Biosystems, Carlsbad, CA) that contained probe and primers for either hENT1, hENT2, hCNT1, hCNT3, dCK, TK1, or ribonucleotide reductase subunit M1 (RRM1) in a final volume of 20 μl/well. Probes and primer for TK1 and RRM1 were purchased as kits from Applied Biosystems (Carlsbad, CA, Assay ID: Hs01062127_g1 and Hs01040706_m1, respectively), while probes and primers were previously described for dCK [22] and for hNTs and glyceraldehyde-3-phosphate dehydrogenase (GAPDH) [19]. Reactions were run in triplicate in 96-well plates using a 7900HT Fast Real-Time PCR system (Applied Biosystems, Carlsbad, CA) using standard default settings. Relative quantification of RNA was determined using the delta–delta C_T method [23] using GAPDH to control for RNA loading differences. The probes and primers for hENT1 displayed an amplification efficiency of 83% (data not shown). When compared to the probes and primers for hENT1, the probes and primers of the other genes displayed no significant differences in amplification efficiencies (data not shown).

2.3. FLT and gemcitabine uptake assays

For all uptake assays, cells in 24-well plates were washed once with PBS [137 mM NaCl (Fisher Scientific, Fair Lawn, NJ), 2.7 mM KCl (Caledon Laboratories Ltd., Georgetown, Canada), 8.1 mM Na_2HPO_4 (BDH Inc., Toronto, Canada), 1.5 mM KH_2PO_4 (BDH Inc., Toronto, Canada)] followed by incubation with DMEM with 10% calf serum (CS) and transport inhibitors (if applicable) for 20 min at 37 °C. Medium was removed and cells were incubated at 37 °C with transport buffer (0.5 ml/well) containing DMEM + 10% FCS with either [^{3}H]FLT or [^{3}H]gemcitabine (Moravek Biochemicals Inc., Brea, CA) as well as transport inhibitors (if applicable). At predetermined time-points, transport buffers were removed and cells were washed three times with PBS. Cells were lysed in wells by addition of KOH (BDH Inc., Toronto, Canada; 0.5 M; 0.5 ml/well) and after incubation for at least 1 h, analyzed for radioactivity by liquid scintillation counting (LS 6500, Beckman Coulter, Fullerton, CA). Incubation of radioactive transport buffers with cells was either for 1 h (tracer uptake is dependent on both transport and phosphorylation) or between 1 and 45 s (tracer uptake is mainly dependent on transport). Transport buffer contained either (i) 100 nM [^{3}H]FLT or [^{3}H]gemcitabine (used for uptake assays with 1-h incubation periods) or (ii) 1 μM [^{3}H]FLT or [^{3}H]gemcitabine (used for uptake assays with 1–45 s incubation periods). Transport inhibitors used in uptake assays included 100 nM NBMPR (Sigma-Aldrich, St. Louis, MO; inhibits only hENT1) and 100 μM dilazep (Sigma–Aldrich, St. Louis, MO; inhibits both hENT1 and hENT2). To determine the role of hCNTs in FLT uptake, assays were performed using 45-s incubation periods with Na^+ buffer [20 mM Tris (Invitrogen, Carlsbad, CA), 3 mM K_2HPO_4, 5 mM glucose (Sigma–Aldrich, St. Louis, MO), and 145 mM NaCl] that contained 1 μM [^{3}H]FLT with or without 1 mM thymidine (Sigma–Aldrich, St. Louis, MO; permeant of hENT1/2 and hCNT1/3), inosine (Sigma–Aldrich, St. Louis, MO; permeant of hENT1/2 and hCNT2/3), or uridine (Sigma–Aldrich, St. Louis, MO; permeant of hENT1/2 and hCNT1/2/3) and 100 μM dilazep (inhibitor of hENT1/2). Protein

content in KOH solutions was determined by the Bio-Rad Protein Assay (Bio-Rad Laboratories, Hercules, CA).

2.4. Equilibrium NBMPR binding assays

Equilibrium NBMPR binding assays using 5-*S*-{2-(1-[(fluorescein-5-yl)thioureido]hexanamido)ethyl}-6-*N*-(4-nitrobenzyl)-5-thioadenosine (FTH-SAENTA, provided by Dr. Morris Robins) to distinguish between intracellular and cell surface binding sites were performed as previously described [19] with slight modifications. The membrane impermeant FTH-SAENTA interacts only with extracellular NBMPR binding sites [24] and thus allows the determination of extracellular NBMPR binding sites, which represent plasma membrane hENT1 molecules. Cells in 24-well plates were washed twice with Na^+ buffer (0.5 ml/well) followed by 1-h incubations with Na^+ buffer (0.5 ml/well) containing 10 nM [^{3}H]NBMPR (Moravek Biochemicals Inc., Brea, CA) alone, 10 nM [^{3}H]NBMPR with 100 nM FTH-SAENTA, or 10 nM [^{3}H]NBMPR with 10 μM non-radioactive NBMPR. Cells were washed three times with Na^+ buffer followed by incubation with 0.5 M KOH for at least 1 h. Cell lysates were analyzed for radioactivity by liquid scintillation counting. Total specifically bound [^{3}H]NBMPR (both extracellular and intracellular) was calculated from the difference between [^{3}H]NBMPR bound in the presence and absence of 10 μM NBMPR. Extracellular specifically bound [^{3}H]NBMPR was calculated from the difference of [^{3}H]NBMPR bound with or without FTH-SAENTA. The percentage of specifically bound extracellular [^{3}H]NBMPR was calculated as (extracellular bound/total bound) × 100.

2.5. Gemcitabine toxicity assays

Gemcitabine toxicity assays were performed using the CellTiter 96® AQ_{ueous} One Solution Cell Proliferation Assay (Promega, Madison, WI). Briefly, 24 h after inoculating cells onto 96-well plates, medium was removed and fresh medium (100 μl/well) with or without graded amounts of gemcitabine (provided by Eli Lilly, Indianapolis, Indiana; final concentrations: 10 pM–100 μM) were added to wells with or without cells. Cells were incubated at 37 °C for 72 h, after which 20 μl [3-(4,5-dimethylthiazol-2-yl)-5-(3-carboxymethoxyphenyl)-2-(4-sulfophenyl)-2H-tetrazolium (MTS) reagent was added to the medium in each well. Plates were shaken on a Titer Plate Shaker (Lab-Line Instruments, Melrose Park, IL) on speed 5 for 15 s and then incubated at 37 °C for up to 4 h. The 490-nm absorbance in each well was determined using a SpectroMAX 190 (Molecular Devices, Sunnyvale, CA) and absorbance values from wells without cells (background) were subtracted from values from wells with cells. Data were analyzed with GraphPad Prism software (version 4.0) using non-linear regression analysis to determine gemcitabine EC_{50} values (concentration that produced 50% of maximum cell death caused by gemcitabine).

2.6. Statistical analysis

Unless otherwise indicated, results were obtained from at least three different experiments with data presented as mean ± SEM. Data were graphed and analyzed using GraphPad Prism (version 4.03) software using default settings and $P < 0.05$ was considered statistically significant.

3. Results

3.1. Quantification of extracellular hENT1 levels with [^{3}H]NBMPR binding

Plasma membrane levels of hENT1 in the six pancreatic cancer cell lines were determined using equilibrium [^{3}H]NBMPR binding assays with or without membrane impermeant FTH-SAENTA or excess non-radioactive NBMPR. Since nucleoside transporters must be on plasma membranes to import nucleosides/nucleoside analogs into cells, quantification of extracellular NBMPR binding sites is more meaningful than quantification of total NBMPR binding sites in assessing hENT1-mediated uptake capacity. Binding of 10 nM [^{3}H]NBMPR with or without 100 nM FTH-SAENTA or 10 μM NBMPR is shown in Fig. 1 for representative experiments conducted with Capan-2 and PANC-1 cells. The difference in [^{3}H]NBMPR binding with and without 10 μM NBMPR represented total specific [^{3}H]NBMPR binding while the difference in [^{3}H]NBMPR binding with and without 100 nM FTH-SAENTA represented cell-surface (i.e., extracellular) specific [^{3}H]NBMPR binding.

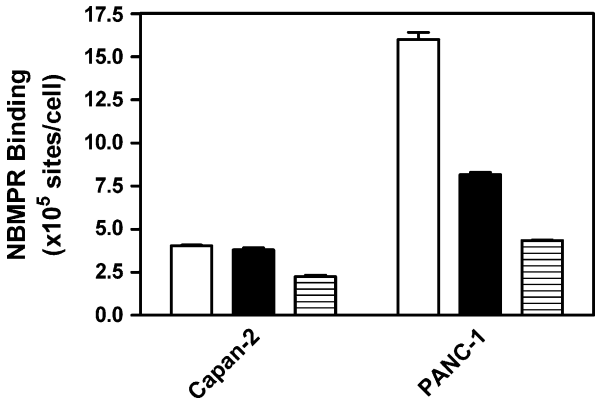

Fig. 1. Binding of 10 nM [^{3}H]NBMPR to Capan-2 and PANC-1 cells in the absence of additives (white bars) or with 100 nM FTH-SAENTA (black bars) or 10 μM non-radioactive NBMPR (striped bars) was measured under equilibrium conditions (1 h, room temperature) as described in Section 2. Shown is a representative experiment performed in triplicate.

Total and extracellular NBMPR binding sites as well as the percentage of extracellular sites are presented in Table 1 for the six cell lines. Capan-2 cells displayed the lowest number of extracellular NBMPR binding sites with 2.1×10^4 sites/cell while AsPC-1, BxPC-3, PL45, MIA PaCa-2, and PANC-1 cells displayed, respectively, 1.4-, 1.6-, 2.6-, 18-, and 35-fold greater extracellular NBMPR binding sites per cell than Capan-2 cells. Less than 30% of the NBMPR binding sites were extracellular for Capan-2, BxPC-3, PL45, and AsPC-1 cells, suggesting that hENT1 was not efficiently transferred to plasma membranes in these cell lines. In contrast, greater than 50% of the NBMPR binding sites were extracellular for MIA PaCa-2 and PANC-1 cells.

3.2. Quantification of relative levels of hNTs, dCK, TK1, and RRM1 mRNA with real-time PCR

A relationship has been shown between gemcitabine resistance and transcript levels of hENT1, dCK, RRM1, and RRM2 in a panel of human pancreatic cancer cell lines [25]. Studies were therefore undertaken using TaqMan real-time PCR to determine transcript levels of hNTs, dCK, TK1, and RRM1 for each cell line and transcript levels were compared to those of hENT1 (Fig. 2A). hENT2 transcript levels were greater than those of hENT1 in BxPC-3 (1.2-fold), Capan-2 (2.9-fold), and AsPC-1 (3.5-fold) cells, while hENT1 transcript levels were greater than those of hENT2 in MIA PaCa-2 (4.6-fold), PANC-1 (7.1-fold), and PL45 (20-fold) cells. For all cell lines, hENT1 transcripts were greater than those of hCNT1 (190- to 6200-fold), hCNT3 (78- to 34000-fold) and dCK (17- to 370-fold), indicating that hENT1 expression was greater than that of hCNTs or dCK. For five of the six cell lines, TK1 expression was greater than that of hENT1 (1.3- to 9.5-fold) whereas PANC-1 cells displayed 1.4-fold greater hENT1 expression than that of TK1. RRM1

transcript levels were greater than those of hENT1 in MIA PaCa-2 (1.3-fold), AsPC-1 (3.4-fold), BxPC-3 (4.5-fold), and Capan-2 (6.7-fold) cells while hENT1 transcript levels were greater than those of RRM1 in PL45 (1.3-fold) and PANC-1 (2.6-fold) cells.

Gene expression levels were also compared between cell lines using Capan-2 cells as the reference (Fig. 2B). hENT1 expression was greatest in PL45 cells (12-fold) followed by PANC-1 (10-fold), MIA PaCa-2 (1.2-fold), Capan-2 (1.0-fold), BxPC-3 (0.65-fold), and AsPC-1 (0.6-fold) cells. The three cell lines with the greatest amount of NBMPR binding sites per cell (PANC-1, MIA PaCa-2, and PL45) in the experiments of Table 1 also displayed the greatest amount of hENT1 expression although the ranking differed. hENT2 expression was greatest in Capan-2 cells (1.0-fold) followed by AsPC-1 (0.72-fold), PANC-1 (0.53-fold), BxPC-3 (0.27-fold), PL45 (0.22-fold), and MIA PaCa-2 (0.09-fold). hCNT1 and hCNT3 expression levels differed between the cell lines although, based on the relative levels of hCNTs as compared to hENTs (see above), the hCNTs probably did not contribute much to FLT or gemcitabine transport in any of the cell lines. Difference in dCK, TK1, and RRM1 expression between cell lines may have led to differences in gemcitabine uptake, FLT uptake, and gemcitabine toxicity, respectively. dCK expression was greatest in Capan-2 cells (1.0-fold) followed by PL45 (0.84-fold), PANC-1 (0.48-fold), AsPC-1 (0.41-fold), BxPC-3 (0.23-fold), and MIA PaCa-2 (0.1-fold) cells. TK1 expression was greatest in PL45 cells (2.6-fold) followed by PANC-1 (1.04-fold), Capan-2 (1.0-fold), BxPC-3 (0.87-fold), AsPC-1 (0.43-fold), and MIA PaCa-2 (0.26-fold) cells. RRM1 expression was greatest in PL45 cells (1.3-fold) followed by Capan-2 (1.0-fold), PANC-1 (0.57-fold), BxPC-3 (0.43-fold), AsPC-1 (0.31-fold), and MIA PaCa-2 (0.22-fold) cells.

3.3. Correlation between FLT and gemcitabine transport in five cell lines

To compare transport of FLT and gemcitabine in the pancreatic cancer cell lines, initial rates of uptake were measured to obtain rates of inward permeation processes under conditions during which there was little or no influence of nucleoside phosphorylation. In an attempt to reproduce physiological conditions, transport buffer consisted of DMEM with 10% CS and assays were conducted at 37 °C rather than the conditions that are commonly used in other cell culture transport assays—i.e., a simplified Na^+ buffer at room temperature. Cultured cells were incubated with 1 μM [^{3}H]FLT or [^{3}H]gemcitabine for short time periods (up to 45 s) in the absence or presence of 100 μM dilazep, and radioactivity in cells was analyzed; representative time courses of uptake of [^{3}H]FLT or [^{3}H]gemcitabine are shown for MIA PaCa-2 cells in Fig. 3A and B. FLT and gemcitabine initial uptake rates were relatively similar, ranging from 24 to 67 and 24 to 42 fmol/mg protein/s, respectively (see Table 2 for summary of data obtained for the six cell lines), with Capan-2 cells displaying the lowest rates of uptake of FLT and gemcitabine. In the presence of 100 μM dilazep, initial rates of uptake of FLT and gemcitabine were 41–55% and 0.3–5% of uninhibited rates, respectively, suggesting that hENT activity was important for uptake of both compounds, although substantial uptake of FLT, but not gemcitabine, also occurred by dilazep-insensitive (i.e., hENT1/2-independent) processes.

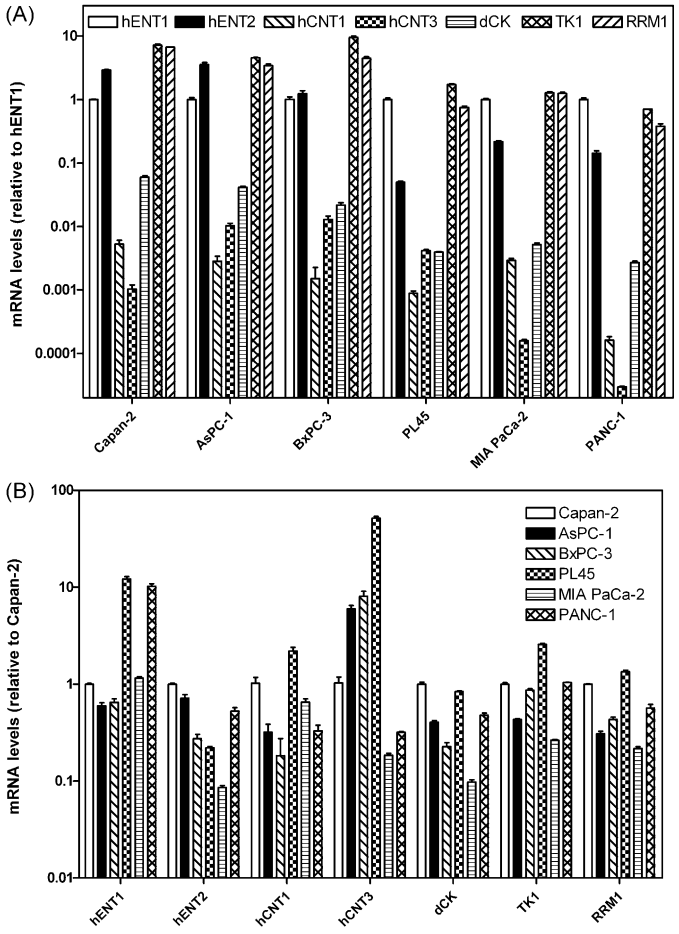

Fig. 2. Quantification of hNT, dCK, TK1, and RRM1 mRNA levels in pancreatic cancer cell lines by real-time PCR. (A) Comparing mRNA levels within each cell line with data normalized to the values for hENT1. Gene analyzed include hENT1 (white bars), hENT2 (black bars), hCNT1 (down-right diagonal striped bars), hCNT3 (square checkered bars), dCK (horizontal striped bars), TK1 (diamond checkered bars) and RRM1 (down-left diagonal striped bars). (B) Comparing mRNA levels between cell lines with data normalized to the values for Capan-2 cells. Cell lines analyzed include Capan-2 (white bars), AsPC-1 (black bars), BxPC-3 (down-right diagonal striped bars), PL45 (square checkered bars), MIA PaCa-2 (horizontal striped bars), and PANC-1 (diamond checkered bars). Relative mRNA levels were determined with the delta–delta C_T method using GAPDH as the loading control and genes were quantified relative to hENT1 mRNA levels as described in Section 2. At least three experiments were performed (each in triplicate) and bars represent mean values ± SEM. Error bars are not shown where they are too small to be distinguished from data bars.

Passive uptake of FLT in BxPC-3 cells was determined by incubating BxPC-3 cells for 45 s with transport buffer containing 1 μM [^{3}H]FLT with or without 1 mM non-radioactive FLT and 100 μM dilazep. The presence of 1 mM non-radioactive FLT and 100 μM dilazep decreased initial rates of FLT uptake to 32% of that without 1 mM FLT and 100 μM dilazep, suggesting that passive diffusion contributed significantly to FLT uptake in BxPC-3 cells (Fig. 3C). Initial rates of FLT uptake in BxPC-3 cells were reduced further when cells were incubated with both 100 μM dilazep and 1 mM FLT compared to that with 100 μM dilazep alone, suggesting that FLT uptake was mediated by at least one other dilazep-insensitive process that was not passive diffusion. When BxPC-3 cells were incubated for 45 s with [^{3}H]FLT and 100 μM dilazep

Table 1
Total and extracellular NBMPR binding sites per cell in pancreatic cancer cell lines. At least three [^{3}H]NBMPR binding experiments were performed under equilibrium conditions (each experiment in triplicate) and data are expressed as mean ± SEM.

Cell line	Total NBMPR	Extracellular NBMPR	
	Binding sites/cell ($\times 10^5$)	Binding sites/cell ($\times 10^5$)	%
Capan-2	1.6 ± 0.3	0.21 ± 0.04	15 ± 4
AsPC-1	1.1 ± 0.1	0.29 ± 0.05	27 ± 4
BxPC-3	2.1 ± 0.1	0.33 ± 0.10	15 ± 5
PL45	2.4 ± 0.4	0.55 ± 0.09	23 ± 2
MIA PaCa-2	6.7 ± 1.0	3.8 ± 0.6	57 ± 6
PANC-1	11 ± 1	7.4 ± 0.5	65 ± 4

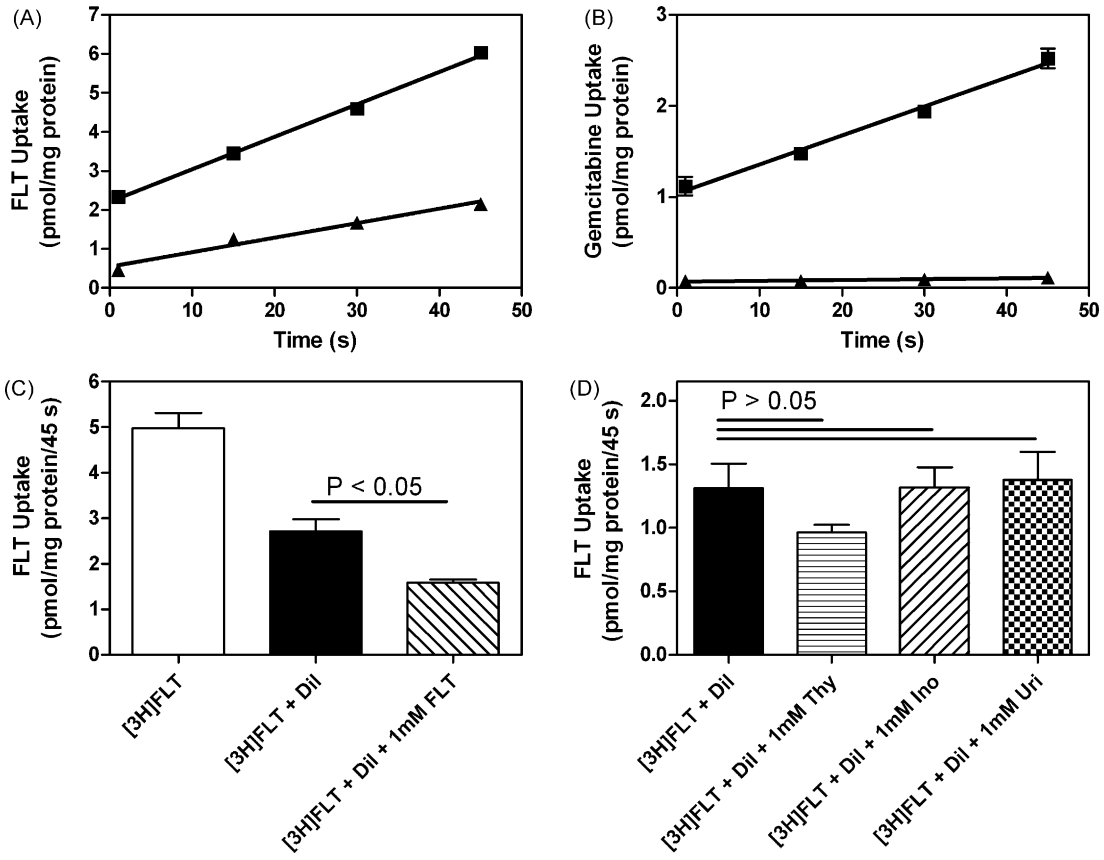

Fig. 3. Initial rates of uptake of 1 μM [^{3}H]FLT (A) or [^{3}H]gemcitabine (B) in MIA PaCa-2 cells. Cells were incubated with [^{3}H]permeant without (squares) or with (triangles) 100 μM dilazep at 37 °C for the indicated times as described in Section 2. Shown are representative experiments performed in triplicate and symbols represent mean uptake values ± SEM. Error bars are not shown when the bars are smaller than the symbols. C, Uptake of 1 μM [^{3}H]FLT into BxPC-3 cells incubated in transport buffer (1) without inhibitors (white bars), (2) with 100 μM dilazep (black bars), or (3) with 100 μM dilazep and 1 mM FLT (diagonal striped bars). D, Uptake of 1 μM [^{3}H]FLT into BxPC-3 cells incubated in transport buffer with 100 μM dilazep (black bars) with 1 mM thymidine (horizontal striped bars), inosine (diagonal striped bars) or uridine (checkered bars). Cells were incubated with transport buffers at 37 °C for 45 s. Experiments were performed three times except those with inosine (n = 2); each experiment was performed in triplicate and bars represent mean values ± SEM.

with or without 1 mM thymidine, inosine or uridine, initial rates of FLT uptake were not significantly affected by the presence of 1 mM non-radioactive nucleosides ($P > 0.05$; Fig. 3D), suggesting that hCNTs were not responsible for the observed hENT1/2-independent FLT uptake.

For all cell lines except one, a significant positive correlation existed between FLT and gemcitabine initial rates of uptake ($P < 0.005$, $r^2 = 0.95$; Fig. 4). BxPC-3 cells displayed a 2.5-fold greater rate of FLT uptake than gemcitabine and therefore did not follow the trend of the other five cell lines. The explanation for this deviation is uncertain.

Table 2
Rates of uptake of FLT and gemcitabine with or without hNT inhibitors between 1 and 45 s in pancreatic cancer cell lines. At least three experiments were performed (each experiment in triplicate) and data are expressed as mean ± SEM.

Cell line	1 μM [^{3}H]FLT (fmol/mg protein/s)		1 μM [^{3}H]gemcitabine (fmol/mg protein/s)	
	No inh.[a]	100 μM Dilazep	No inh.	100 μM dilazep
Capan-2	24 ± 1	12 ± 2	24 ± 2	1.2 ± 0.4
AsPC-1	40 ± 4	22 ± 2	32 ± 6	1.2 ± 0.7
BxPC-3	67 ± 7	31 ± 6	27 ± 2	0.2 ± 0.1
PL45	39 ± 7	16 ± 3	35 ± 7	0.1 ± 0.1
MIA PaCa-2	59 ± 5	31 ± 3	41 ± 5	0.8 ± 0.4
PANC-1	57 ± 5	28 ± 3	42 ± 4	0.7 ± 0.3

[a] no inh. means no hNT inhibitor used in transport assays.

3.4. Dependence of FLT and gemcitabine uptake on hNT activity

During prolonged exposures to nucleoside analogs such as FLT and gemcitabine, uptake represents the combined effects of permeation through plasma membranes and intracellular

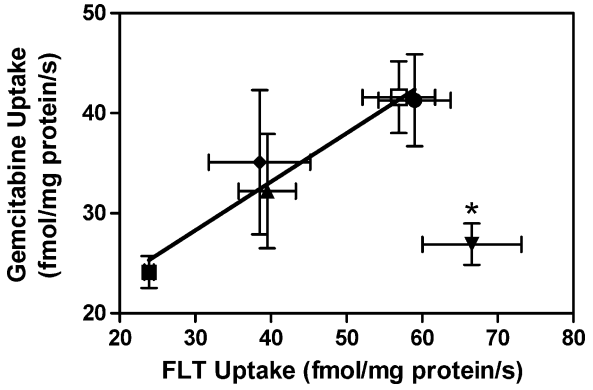

Fig. 4. Linear regression analysis of FLT and gemcitabine initial rates of uptake in Capan-2 (■), AsPC-1 (▲), PL45 (◆), MIA PaCa-2 (●), and PANC-1 (□) cells. Data were taken from Table 2 for FLT and gemcitabine transport in the absence of hNT inhibitors and symbols represent mean values ± SEM. For the five cell lines included in the analysis, a significant positive correlation existed between FLT and gemcitabine transport ($P < 0.005$, $r^2 = 0.95$). BxPC-3 cells, indicated with the asterisk, were not included in the linear regression analysis.

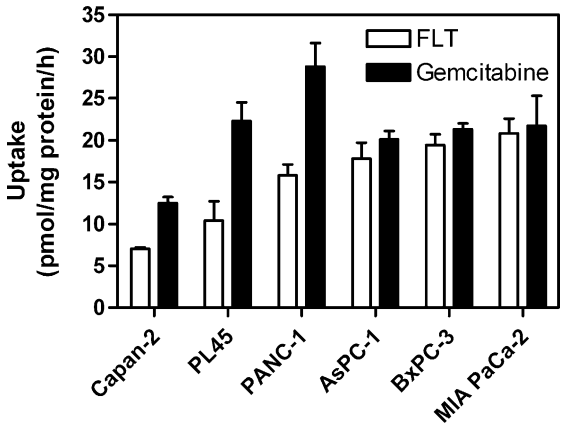

Fig. 5. Uptake of 100 nM [^{3}H]FLT and [^{3}H]gemcitabine in pancreatic cancer cell lines. Cells were incubated with [^{3}H]FLT (white bars) or [^{3}H]gemcitabine (black bars) at 37 °C for 1 h as described in Section 2. At least three experiments were performed (each in triplicate) and bars represent mean uptake values ± SEM. Error bars are not shown where they are too small to be distinguished from data bars.

nucleoside phosphorylation. In the experiments of Fig. 5, uptake of 100 nM [^{3}H]FLT and [^{3}H]gemcitabine was measured after 1-h incubations to assess the impact of nucleoside phosphorylation. For the six pancreatic cell lines, FLT and gemcitabine uptake values ranged from 7 to 21 and 13 to 29 pmol/mg protein/h, respectively, with Capan-2 cells displaying the lowest values (Table 3), which was surprising given their high levels of dCK and TK1 mRNA (Fig. 2). When comparing all cell lines, there were no positive correlations between (1) TK1 expression and FLT uptake, or (2) dCK expression and gemcitabine uptake. In the presence of 100 nM NBMPR, FLT and gemcitabine uptake values were 27–74% and 7–24% of uninhibited values, respectively, suggesting that hENT1 activity affected both FLT and gemcitabine uptake but was more important for gemcitabine than for FLT. In the presence of 100 μM dilazep, which inhibits both hENT1 and hENT2 activities, FLT and gemcitabine uptake values were reduced even further, to 12–58% and 1–2% of uninhibited values, respectively. As was the case with inhibition of hENT1 activity, the effect of inhibition of hENT1/2 activities was greater for gemcitabine than for FLT.

3.5. Dependence of gemcitabine toxicity on hNT activity

The sensitivities of the pancreatic cancer cell lines to gemcitabine cytotoxicity were determined using the Promega CellTiter 96® AQ_{ueous} One Solution Cell Proliferation Assay. Cells were incubated with graded concentrations of gemcitabine with or without 100 nM NBMPR or 10 μM dilazep for 72 h to determine if hENT activity affected gemcitabine toxicity. Results for all cell lines are summarized in Table 4. Capan-2 cells displayed the greatest EC_{50} value (gemcitabine concentration that produced 50% of maximal effect) at 3500 nM, with lower values exhibited by PANC-1 (820 nM), PL45 (53 nM), AsPC-1 (39 nM), BxPC-3 (27 nM), and MIA PaCa-2 (8.3 nM) cells. Addition of 100 nM NBMPR increased gemcitabine EC_{50} values 1.3- to 7.7-fold for all cell lines except PANC-1, which displayed gemcitabine EC_{50} values that were not significantly different with or without NBMPR ($P > 0.05$). Addition of 10 μM dilazep increased gemcitabine EC_{50} values 2.1- to 41-fold for all cell lines including PANC-1, suggesting that hENT1 and hENT2 activity was important for gemcitabine toxicity since inhibition of both hENT1 and hENT2 caused greater gemcitabine resistance than inhibition of only hENT1.

3.6. Correlations between gemcitabine uptake, FLT uptake, or RRM1 expression and gemcitabine toxicity in five cell lines

To determine if FLT uptake could be used to predict gemcitabine toxicity in the pancreatic cancer cell lines, FLT uptake with 1 h tracer incubation and gemcitabine toxicity data were analyzed since FLT PET scans in human patients are typically up to 1 h after tracer injection. Gemcitabine uptake correlated negatively with gemcitabine resistance for all cell lines except PANC-1 ($P < 0.005$, $r^2 = 0.96$; Fig. 6A), which did not fit the trend since it displayed the greatest amount of gemcitabine uptake but was the second most gemcitabine resistant. FLT uptake also displayed a significant negative correlation with gemcitabine resistance for five of the six cell lines ($P < 0.005$, $r^2 = 0.96$; Fig. 6B), although the cell line that did not fit the trend was PL45. The gemcitabine EC_{50} value was similar to that of AsPC-1 cells, whereas FLT uptake after 1 h was approximately only half of that of AsPC-1 cells. Interestingly, RRM1 expression also correlated positively with gemcitabine resistance ($P < 0.01$) when PL45 cells were excluded from analysis (Fig. 6C). Compared to the other cell lines, PL45 displayed the greatest expression of RRM1 (Fig. 2B) but was still relatively sensitive to gemcitabine (Table 4).

4. Discussion

Clinical resistance to gemcitabine has been relatively well studied. hNTs are necessary for gemcitabine transport into tumor cells and a lack of hNT activity, especially hENT1, leads to gemcitabine resistance in cultured cell lines and pancreatic cancer patients [3–5]. dCK is the rate limiting enzyme in the phosphorylation of gemcitabine, which is necessary for the pharmacologic activation of gemcitabine, and decreased dCK protein levels correlates with gemcitabine resistance [26,27]. RRM1 is also considered to be important in gemcitabine resistance since increased expression of RRM1 mRNA is associated with gemcitabine resistance [28,29]. In the current study, if PL45 cells were excluded from analysis, RRM1 expression positively correlated with gemcitabine resistance ($P < 0.01$), suggesting that RRM1 levels may also be useful to predict gemcitabine sensitivity. Predicting response of pancreatic cancer patients to gemcitabine has been achieved by assessing hENT1 abundance by immunohistochemistry on pancreatic tumors obtained at surgery [4].

Table 3
FLT and gemcitabine uptake with or without hNT inhibitors after 1 h in pancreatic cancer cell lines. At least three experiments were performed (each experiment in triplicate) and data are expressed as mean ± SEM.

Cell line	100 nM [^{3}H]FLT (pmol/mg protein/h)			100 nM [^{3}H]gemcitabine (pmol/mg protein/h)		
	No inh.[a]	100 nM NBMPR	100 μM dilazep	No inh.	100 nM NBMPR	100 μM dilazep
Capan-2	7.0 ± 0.2	4.9 ± 0.2	2.9 ± 0.2	13 ± 0.7	3.1 ± 0.2	0.16 ± 0.01
AsPC-1	18 ± 2	11 ± 0.4	7.9 ± 0.4	20 ± 1	3.6 ± 0.2	0.23 ± 0.02
BxPC-3	19 ± 1	14 ± 1	11 ± 1	21 ± 0.7	4.0 ± 0.4	0.17 ± 0.01
PL45	10 ± 2	2.7 ± 0.6	1.2 ± 0.3	22 ± 2	1.6 ± 0.2	0.30 ± 0.06
MIA PaCa-2	21 ± 2	10 ± 1	4.8 ± 0.6	22 ± 4	2.8 ± 0.3	0.23 ± 0.05
PANC-1	16 ± 1	6.5 ± 0.8	5.7 ± 0.7	29 ± 3	2.2 ± 0.3	0.15 ± 0.01

[a] No inh. means no hNT inhibitor used in uptake assays.

Table 4
Gemcitabine toxicity with or without hNT inhibitors in pancreatic cancer cell lines. At least three experiments were performed (each experiment in triplicate) and data are expressed as mean ± SEM.

Cell line	Gemcitabine EC_{50} values (nM)		
	No inh.[a]	100 nM NBMPR	10 μM dilazep
Capan-2	3500 ± 400	4600 ± 1700	7500 ± 1600
AsPC-1	39 ± 5	300 ± 80	510 ± 30
BxPC-3	27 ± 7	75 ± 10	180 ± 20
PL45	53 ± 10	290 ± 60	930 ± 70
MIA PaCa-2	8.3 ± 2.4	19 ± 0.9	340 ± 50
PANC-1	820 ± 150	560 ± 90	5000 ± 400

[a] No inh. means no hNT inhibitor used in toxicity assays.

Unfortunately, only 10–15% of pancreatic cancer patients are eligible for tumor resection [1], and a non-invasive assay is, therefore, necessary to predict response to gemcitabine for the majority of pancreatic cancer patients. Uptake of the recently developed PET tracer 1-(2′-deoxy-2′-fluoroarabinofuranosyl) cytosine (FAC), which is a dCK substrate, was used to determine tumor dCK activity (since FAC uptake is dependent on dCK activity) and predict gemcitabine toxicity in L1210 tumor-bearing mice [30]. The current study assessed if uptake of the clinically available PET tracer FLT predicts gemcitabine toxicity in pancreatic cancer cell lines since FLT and gemcitabine are transported by the same hNTs.

Using an inhibitor-sensitivity assay in hNT-producing *Saccharomyces cerevisiae*, K_i values were previously calculated from concentrations that caused 50% inhibition of uridine transport for FLT and gemcitabine, respectively, for hENT1 (74 and 354 μM), hENT2 (160 and 780 μM), hCNT1 (20 and 13 μM), hCNT2 (1200 and 1320 μM), and hCNT3 (31 and 22 μM) [19,31]. The data indicated that hENTs have higher affinities for FLT than gemcitabine whereas hCNTs have very similar affinities for both FLT and gemcitabine. Thus, although FLT and gemcitabine are permeants for the same hNTs (hENT1/2 and hCNT1/3), differences between them in individual hNT transport efficiencies will likely be reflected in differences in hNT transport rates in a particular cell type.

In the current study, hENT1 and hENT2 were shown to be important for gemcitabine and FLT uptake and gemcitabine toxicity since co-incubation with NBMPR or dilazep significantly reduced gemcitabine and FLT uptake and increased gemcitabine resistance in the six pancreatic cancer cell lines tested. Capan-2 cells displayed the lowest amount of (1) extracellular NBMPR binding sites, (2) FLT and gemcitabine uptake, and (3) gemcitabine sensitivity. It should be noted that the amount and percent of extracellular NBMPR binding sites for Capan-2 were larger in this study than those previously reported [19] although total NBMPR binding sites per cell were relatively similar.[1] Capan-2 cells were cultured differently in the two studies[2] and this may have caused changes in the Capan-2 cell cycle during experiments, since plasma membrane levels of hENT1 are cell cycle-dependent [32]. Immunofluorescence microscopy using antibodies against hENT1 with Capan-2 cells suggested that approximately 10% of hENT1 was on plasma membranes (data not shown), which was similar to the observed value of 15% for extracellular NBMPR binding in the present study.

In five of six pancreatic cancer cell lines, a positive correlation existed between FLT and gemcitabine transport, as measured by initial rates of uptake. BxPC-3 cells did not fit the trend of the other cell lines since FLT transport was significantly greater than that of gemcitabine. BxPC-3 cells displayed significant levels of FLT passive diffusion. The octanol–water partition coefficients for FLT and gemcitabine are 0.68 [33] and 0.053 (Gemcitabine Hydrochloride for Injection Material Safety Data Sheet), respectively, indicating that FLT is significantly more hydrophobic than gemcitabine, thereby explaining the greater level of passive diffusion observed with FLT than with gemcitabine. Although passive diffusion of FLT in BxPC-3 cells was relatively large compared to that of gemcitabine, diffusional FLT uptake was relatively small compared to mediated FLT uptake, indicating the importance of hNTs in cellular uptake of FLT.

FLT and gemcitabine are phosphorylated by TK1 and dCK, respectively, and these differences in nucleoside phosphorylation

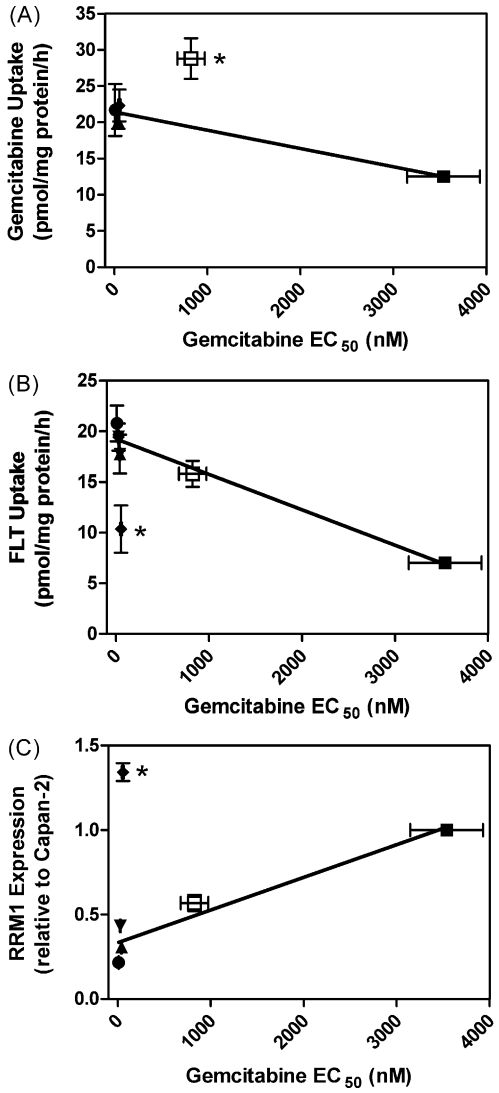

Fig. 6. Linear regression analysis of gemcitabine toxicity in pancreatic cell lines with (A) gemcitabine uptake, (B) FLT uptake, or (C) RRM1 expression. Data were taken from Table 3 (FLT and gemcitabine uptake), Fig. 2B (RRM1 expression) and Table 4 (gemcitabine toxicity) and symbols represent mean values ± SEM. (A) For the five cell lines included in the analysis [Capan-2 (■), AsPC-1 (▲), BxPC-3 (▼), PL45 (◆), and MIA PaCa-2 (●)], significant correlations existed between gemcitabine resistance and gemcitabine uptake ($P < 0.005$, $r^2 = 0.96$). PANC-1 cells, indicated with the asterisk, were not included in the linear regression analysis. (B and C) For the five cell lines included in the analysis [Capan-2 (■), AsPC-1 (▲), BxPC-3 (▼), MIA PaCa-2 (●), and PANC-1 (□)], significant correlations existed between gemcitabine resistance and (1) FLT uptake ($P < 0.005$, $r^2 = 0.96$) and (2) RRM1 expression ($P < 0.01$, $r^2 = 0.92$). PL45 cells, indicated with the asterisk, were not included in the linear regression analysis.

[1] In the previous study, Capan-2 had (i) $1.1 \times 10^5 \pm 0.2 \times 10^5$ total specific NBMPR binding sites/cell, (ii) $0.02 \times 10^5 \pm 0.002 \times 10^5$ extracellular NBMPR binding sites/cell, and (iii) 1.6 ± 1.6% extracellular NBMPR binding sites.

[2] In the previous study, 12-well plates were inoculated with 5×10^4 cells/well and experiments were performed 72 h later.

may also cause differences in cellular uptake between FLT and gemcitabine. Tumor cells with low TK1 and high dCK activities would be expected to display relatively low and high levels of FLT and gemcitabine uptake, respectively. However, PL45 cells, which had low and high levels of FLT and gemcitabine uptake, respectively, displayed greater TK1 than dCK expression (Fig. 2A). Compared to the other cell lines, PL45 displayed relatively high expression of several genes including the greatest expression of hENT1 even though they had only moderate levels of NBMPR binding sites (representing hENT1 molecules, Table 1), suggesting that transcript levels in PL45 cells may not reflect protein levels.

A significant negative correlation was observed between gemcitabine uptake and resistance in only five of six cell lines, suggesting that uptake analysis of any nucleoside analog, including gemcitabine, FAC or FLT, will never be 100% accurate for predicting gemcitabine toxicity since gemcitabine toxicity is dependent on more than just gemcitabine transport and phosphorylation. Although a perfect correlation was not observed between FLT uptake and gemcitabine resistance for the six pancreatic cancer cell lines included in this study, the results suggested that FLT PET could be used to identify pancreatic tumors with low gemcitabine transport capacity that would thus be resistant to gemcitabine therapy. hENT1 immunohistochemistry has proven to be a clinical predictive assay for gemcitabine response in pancreatic cancer even though the assay only monitors the abundance of a single hNT [4]. FLT PET may provide *functional* data on the combined transport capacities of hENT1, hENT2, hCNT1, and hCNT3—i.e., all of the hNTs known to transport gemcitabine. Pancreatic tumors with high FLT uptake are expected to have hNTs capable of FLT transport and are likely to be similar to pancreatic tumors that were positive by immunohistochemistry for hENT1 in the Farrell et al. study [4]. In the current study, the three cell lines with the highest amount of FLT uptake were also the three most sensitive to gemcitabine (Tables 3 and 4). When using hENT1 immunohistochemistry, 44 of 198 (22%) of pancreatic tumors had no detectable hENT1 and patients with these tumors displayed the lowest overall survival rates when taking gemcitabine [4]. Clinical [^{18}F]FLT PET of pancreatic cancers have shown that a similar percentage of pancreatic cancers (6 of 21; 29%) do not display focally increased [^{18}F]FLT uptake [34], suggesting that tumors with no focally increased [^{18}F]FLT uptake may have low/no hENT1 and would not respond well to gemcitabine.

FLT uptake is dependent on the proportion of cells in S-phase [35,36] and gemcitabine toxicity is also partly dependent on cells cycling through S-phase since gemcitabine-induced DNA fragmentation and toxicity are both enhanced when cells are in S-phase [37,38]. Furthermore, levels of gemcitabine-triphosphate incorporation into DNA are positively correlated with gemcitabine toxicity [39], suggesting that incorporation of gemcitabine into DNA is an important process for gemcitabine toxicity. Since both FLT uptake and gemcitabine toxicity are directly related to the proportion of cells in S-phase, monitoring tumor proliferative status with FLT PET may help predict which tumors are sensitive to gemcitabine. Theoretically, this is another reason why FLT uptake may predict gemcitabine toxicity although further studies are necessary to validate this hypothesis.

FLT PET is capable of distinguishing between benign and malignant pancreatic tumors since focal uptake of [^{18}F]FLT was observed exclusively in malignant pancreatic tumors [34]. The current study provides an additional reason for performing FLT PET on untreated pancreatic cancer patients since FLT uptake may also predict gemcitabine sensitivity in pancreatic tumors. Performing FLT PET after gemcitabine therapy may also indicate response to therapy since gemcitabine causes an accumulation of cells in early S-phase, causing an increase in FLT uptake [40]. Therefore, future clinical studies should examine FLT PET images of pancreatic tumors before and after gemcitabine treatment since both may be useful for predicting gemcitabine response.

In summary, the current study demonstrated that gemcitabine and FLT uptake in human pancreatic cancer cell lines was dependent on hNT activities and that FLT and gemcitabine uptake were comparable for predicting gemcitabine toxicity. Future FLT PET clinical trials of pancreatic cancer patients are warranted to determine the potential of FLT PET in predicting tumor gemcitabine sensitivity.

Acknowledgements

This work was supported by research grants from Canadian Cancer Society Research Institute, the Alberta Cancer Research Institute, and the Canadian Institutes of Health Research. R.J.P. and J.D.Y. are, respectively, recipients of Graduate Studentship and Heritage Scientist awards from the Alberta Heritage Foundation for Medical Research.

References

[1] Cartwright T, Richards DA, Boehm KA. Cancer of the pancreas: are we making progress? A review of studies in the US Oncology Research Network. Cancer Control 2008;15:308–13.
[2] Moore MJ, Goldstein D, Hamm J, Figer A, Hecht JR, Gallinger S, et al. Erlotinib plus gemcitabine compared with gemcitabine alone in patients with advanced pancreatic cancer: a phase III trial of the National Cancer Institute of Canada Clinical Trials Group. J Clin Oncol 2007;25:1960–6.
[3] Mackey JR, Mani RS, Selner M, Mowles D, Young JD, Belt JA, et al. Functional nucleoside transporters are required for gemcitabine influx and manifestation of toxicity in cancer cell lines. Cancer Res 1998;58:4349–57.
[4] Farrell JJ, Elsaleh H, Garcia M, Lai R, Ammar A, Regine WF, et al. Human equilibrative nucleoside transporter 1 levels predict response to gemcitabine in patients with pancreatic cancer. Gastroenterology 2009;136:187–95.
[5] Spratlin J, Sangha R, Glubrecht D, Dabbagh L, Young JD, Dumontet C, et al. The absence of human equilibrative nucleoside transporter 1 is associated with reduced survival in patients with gemcitabine-treated pancreas adenocarcinoma. Clin Cancer Res 2004;10:6956–61.
[6] Kong W, Engel K, Wang J. Mammalian nucleoside transporters. Curr Drug Metab 2004;5:63–84.
[7] Molina-Arcas M, Trigueros-Motos L, Casado FJ, Pastor-Anglada M. Physiological and pharmacological roles of nucleoside transporter proteins. Nucleosides Nucleotides Nucleic Acids 2008;27:769–78.
[8] Young JD, Yao SY, Sun L, Cass CE, Baldwin SA. Human equilibrative nucleoside transporter (ENT) family of nucleoside and nucleobase transporter proteins. Xenobiotica 2008;38:995–1021.
[9] Baldwin SA, Yao SY, Hyde RJ, Ng AM, Foppolo S, Barnes K, et al. Functional characterization of novel human and mouse equilibrative nucleoside transporters (hENT3 and mENT3) located in intracellular membranes. J Biol Chem 2005;280:15880–7.
[10] Barnes K, Dobrzynski H, Foppolo S, Beal PR, Ismat F, Scullion ER, et al. Distribution and functional characterization of equilibrative nucleoside transporter-4, a novel cardiac adenosine transporter activated at acidic pH. Circ Res 2006;99:510–9.
[11] Griffiths M, Beaumont N, Yao SY, Sundaram M, Boumah CE, Davies A, et al. Cloning of a human nucleoside transporter implicated in the cellular uptake of adenosine and chemotherapeutic drugs. Nat Med 1997;3:89–93.
[12] Griffiths M, Yao SY, Abidi F, Phillips SE, Cass CE, Young JD, et al. Molecular cloning and characterization of a nitrobenzylthioinosine-insensitive (ei) equilibrative nucleoside transporter from human placenta. Biochem J 1997;328(Pt 3):739–43.
[13] Mackey JR, Yao SY, Smith KM, Karpinski E, Baldwin SA, Cass CE, et al. Gemcitabine transport in xenopus oocytes expressing recombinant plasma membrane mammalian nucleoside transporters. J Natl Cancer Inst 1999;91:1876–81.
[14] Govindarajan R, Leung GP, Zhou M, Tse CM, Wang J, Unadkat JD. Facilitated mitochondrial import of anti-viral and anti-cancer nucleoside drugs by human equilibrative nucleoside transporter-3 (hENT3). Am J Physiol Gastrointest Liver Physiol 2009.
[15] Ritzel MW, Ng AM, Yao SY, Graham K, Loewen SK, Smith KM, et al. Molecular identification and characterization of novel human and mouse concentrative Na+-nucleoside cotransporter proteins (hCNT3 and mCNT3) broadly selective for purine and pyrimidine nucleosides (system cib). J Biol Chem 2001;276:2914–27.
[16] Ritzel MW, Yao SY, Huang MY, Elliott JF, Cass CE, Young JD. Molecular cloning and functional expression of cDNAs encoding a human Na+-nucleoside cotransporter (hCNT1). Am J Physiol 1997;272:C707–14.

[17] Wang J, Su SF, Dresser MJ, Schaner ME, Washington CB, Giacomini KM. Na(+)-dependent purine nucleoside transporter from human kidney: cloning and functional characterization. Am J Physiol 1997;273:F1058–65.
[18] Hu H, Endres CJ, Chang C, Umapathy NS, Lee EW, Fei YJ, et al. Electrophysiological characterization and modeling of the structure activity relationship of the human concentrative nucleoside transporter 3 (hCNT3). Mol Pharmacol 2006;69:1542–53.
[19] Paproski RJ, Ng AM, Yao SY, Graham K, Young JD, Cass CE. The role of human nucleoside transporters in uptake of 3′-deoxy-3′-fluorothymidine. Mol Pharmacol 2008;74:1372–80.
[20] Arner ES, Eriksson S. Mammalian deoxyribonucleoside kinases. Pharmacol Ther 1995;67:155–86.
[21] Been LB, Suurmeijer AJ, Cobben DC, Jager PL, Hoekstra HJ, Elsinga PH. [18F]FLT-PET in oncology: current status and opportunities. Eur J Nucl Med Mol Imaging 2004;31:1659–72.
[22] Mackey JR, Galmarini CM, Graham KA, Joy AA, Delmer A, Dabbagh L, et al. Quantitative analysis of nucleoside transporter and metabolism gene expression in chronic lymphocytic leukemia (CLL): identification of fludarabine-sensitive and -insensitive populations. Blood 2005;105:767–74.
[23] Livak KJ, Schmittgen TD. Analysis of relative gene expression data using real-time quantitative PCR and the 2(−Delta Delta C(T)) method. Methods 2001;25:402–8.
[24] Visser F, Sun L, Damaraju V, Tackaberry T, Peng Y, Robins MJ, et al. Residues 334 and 338 in transmembrane segment 8 of human equilibrative nucleoside transporter 1 are important determinants of inhibitor sensitivity, protein folding, and catalytic turnover. J Biol Chem 2007;282:14148–57.
[25] Nakano Y, Tanno S, Koizumi K, Nishikawa T, Nakamura K, Minoguchi M, et al. Gemcitabine chemoresistance and molecular markers associated with gemcitabine transport and metabolism in human pancreatic cancer cells. Br J Cancer 2007;96:457–63.
[26] Ruiz van Haperen VW, Veerman G, Eriksson S, Boven E, Stegmann AP, Hermsen M, et al. Development and molecular characterization of a 2′,2′-difluorodeoxycytidine-resistant variant of the human ovarian carcinoma cell line A2780. Cancer Res 1994;54:4138–43.
[27] Sebastiani V, Ricci F, Rubio-Viqueira B, Kulesza P, Yeo CJ, Hidalgo M, et al. Immunohistochemical and genetic evaluation of deoxycytidine kinase in pancreatic cancer: relationship to molecular mechanisms of gemcitabine resistance and survival. Clin Cancer Res 2006;12:2492–7.
[28] Bepler G, Kusmartseva I, Sharma S, Gautam A, Cantor A, Sharma A, et al. RRM1 modulated in vitro and in vivo efficacy of gemcitabine and platinum in non-small-cell lung cancer. J Clin Oncol 2006;24:4731–7.
[29] Rosell R, Danenberg KD, Alberola V, Bepler G, Sanchez JJ, Camps C, et al. Ribonucleotide reductase messenger RNA expression and survival in gemcitabine/cisplatin-treated advanced non-small cell lung cancer patients. Clin Cancer Res 2004;10:1318–25.
[30] Laing RE, Walter MA, Campbell DO, Herschman HR, Satyamurthy N, Phelps ME, et al. Noninvasive prediction of tumor responses to gemcitabine using positron emission tomography. Proc Natl Acad Sci U S A 2009;106:2847–52.
[31] Clarke ML, Damaraju VL, Zhang J, Mowles D, Tackaberry T, Lang T, et al. The role of human nucleoside transporters in cellular uptake of 4′-thio-beta-D-arabinofuranosylcytosine and beta-D-arabinosylcytosine. Mol Pharmacol 2006;70:303–10.
[32] Pressacco J, Wiley JS, Jamieson GP, Erlichman C, Hedley DW. Modulation of the equilibrative nucleoside transporter by inhibitors of DNA synthesis. Br J Cancer 1995;72:939–42.
[33] Schinazi RF, Boudinot FD, Doshi KJ, McClure HM. Pharmacokinetics of 3′-fluoro-3′-deoxythymidine and 3′-deoxy-2′,3′-didehydrothymidine in rhesus monkeys. Antimicrob Agents Chemother 1990;34:1214–9.
[34] Herrmann K, Eckel F, Schmidt S, Scheidhauer K, Krause BJ, Kleeff J, et al. In vivo characterization of proliferation for discriminating cancer from pancreatic pseudotumors. J Nucl Med 2008;49:1437–44.
[35] Rasey JS, Grierson JR, Wiens LW, Kolb PD, Schwartz JL. Validation of FLT uptake as a measure of thymidine kinase-1 activity in A549 carcinoma cells. J Nucl Med 2002;43:1210–7.
[36] Schwartz JL, Tamura Y, Jordan R, Grierson JR, Krohn KA. Monitoring tumor cell proliferation by targeting DNA synthetic processes with thymidine and thymidine analogs. J Nucl Med 2003;44:2027–32.
[37] Huang P, Plunkett W. Induction of apoptosis by gemcitabine. Semin Oncol 1995;22:19–25.
[38] Huang P, Plunkett W. Fludarabine- and gemcitabine-induced apoptosis: incorporation of analogs into DNA is a critical event. Cancer Chemother Pharmacol 1995;36:181–8.
[39] Veltkamp SA, Pluim D, van Eijndhoven MA, Bolijn MJ, Ong FH, Govindarajan R, et al. New insights into the pharmacology and cytotoxicity of gemcitabine and 2′,2′-difluorodeoxyuridine. Mol Cancer Ther 2008;7:2415–25.
[40] Dittmann H, Dohmen BM, Kehlbach R, Bartusek G, Pritzkow M, Sarbia M, et al. Early changes in [18F]FLT uptake after chemotherapy: an experimental study. Eur J Nucl Med Mol Imaging 2002;29:1462–9.